

Problems in digital microscopy

C.A. Glasbey

Biomathematics and Statistics Scotland

JCMB, King's Buildings, Edinburgh EH9 3JZ, Scotland

Three case studies are used to illustrate some issues which arise when digital image analysis methods are applied in microscopy. An algorithm is described for estimating the diameters of cashmere fibres from out-of-focus images. The process of image formation in differential interference contrast (DIC) microscopy is modelled, and used to construct templates for identifying and measuring algal, bacterial and fungal cells. Finally, the three-dimensional structure of a diatom is recovered by analysing images from a series of focal planes.

Introduction

Sight is fundamental to our understanding of the world. This is as true in the biological sciences as in everyday life, and the collection of much biometric data is dependent on human vision. For example, the examination of samples under a microscope, the observing of animal behaviour, and the identification and counting of plant species in a field are all forms of image analysis. The human vision system is superb – we see effortlessly, though it uses up one-third of our brains. However, computers are increasingly being used to automate and extend the potential of image analysis (see, e.g., Glasbey and Horgan, 1995, and [http:// www.bioss.sari.ac.uk/BioSS/ Research/ image.html](http://www.bioss.sari.ac.uk/BioSS/Research/image.html)). The reasons are that computers can do better than human observers at extracting quantitative information from images, and they can spare us from a lot of routine image interpretation.

In the past twenty years, much effort worldwide has been spent in developing image processing algorithms for applications such as robot vision, medical scanning systems and satellite remote sensing. In comparison, and with some noteworthy exceptions, the development of algorithms specific to microscopy has been neglected. Generic image processing algorithms are often applied successfully, but they fail to exploit fully the information contained in microscope images. There is also a danger of misinterpretation if the optics which produced a particular image are not correctly understood. For example, the bas-relief type of images typical of DIC microscopy (see Figure 1) may be mistaken for three-dimensional features. Tailoring image processing algorithms to particular forms of microscopy poses a considerable challenge. There are many optical microscope systems, including brightfield, darkfield, phase contrast, interference

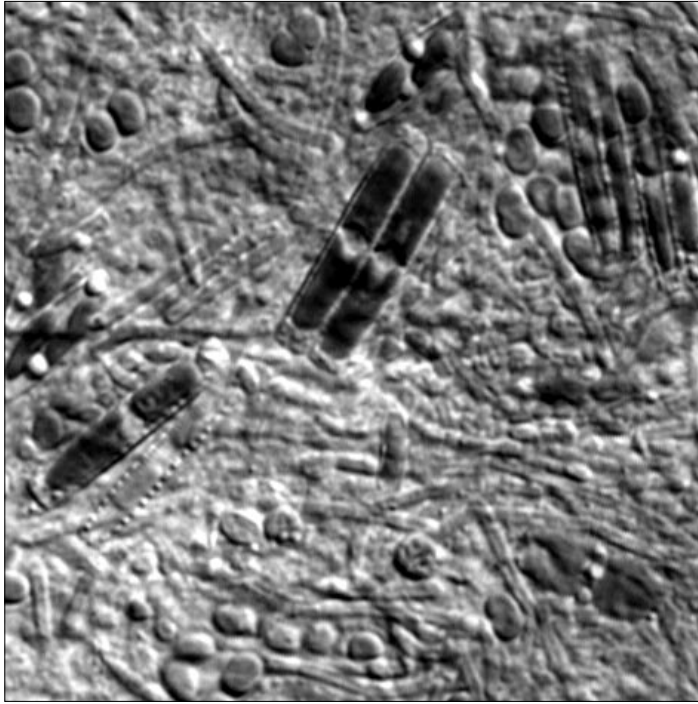


Figure 1: *Differential interference contrast microscope image of a mixed population of algal cells.*

contrast, fluorescence and confocal systems (see, e.g., Slayter and Slayter, 1992). Further, the theory of microscopy is complicated and agreement with data is less than perfect. The challenge is to synthesise theoretical models and empirical evidence in order to tackle particular image analysis problems. Some of these problems will be illustrated by considering three examples, as follows.

Becke lines

Figure 2 shows a back-illuminated brightfield microscope image of cashmere goat fibres, obtained in order to measure the fibre diameters. All the fibres should appear the same, but they don't. The microscope is at high magnification and so has a shallow depth of focus. Some fibres are out of focus, and this gives rise to *Becke lines* – either dark or light edges to the fibres. It is important to take these edges into account, both in locating the fibres in the image and in measuring their diameters.

Glasbey *et al.* (1994) showed that Becke lines edges are produced by the fibres acting as lenses which refract the light passing through them. To illustrate, Figure 3 shows the mathematically-derived appearance of an idealised fibre viewed at a slightly tilted angle so that it passes through the focal plane of the microscope. On the left the fibre is below the focal plane and appears to have white edges, whereas on the right the fibre is above the focal plane and appears to have black edges. We found that although the mathematical model was sufficient for gaining a

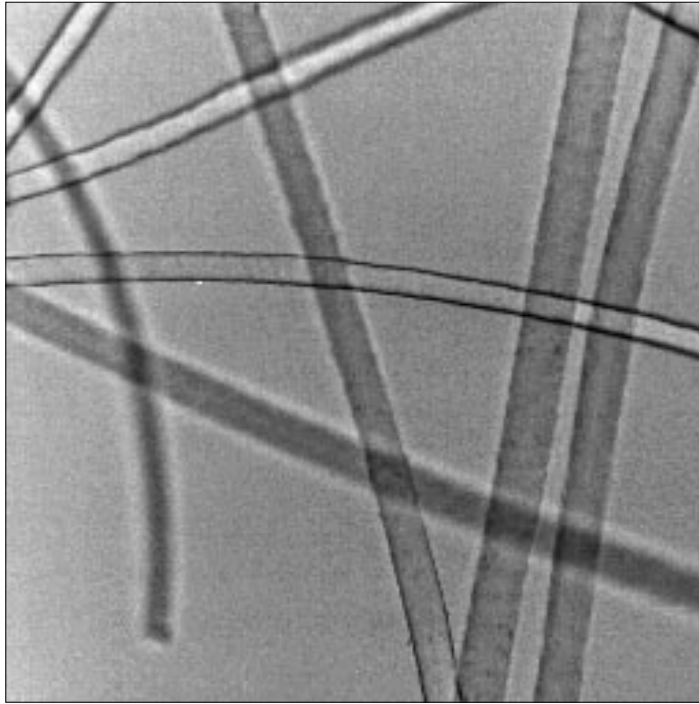


Figure 2: *Brightfield microscope image of cashmere goat fibres.*

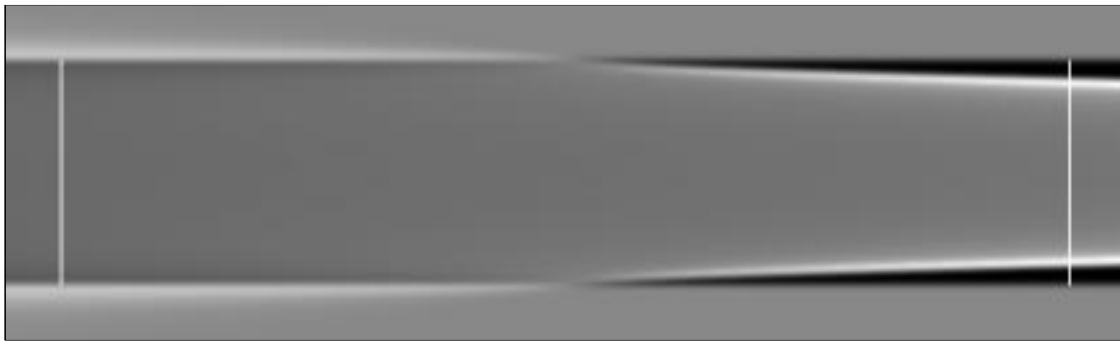


Figure 3: *An idealised fibre viewed at a slightly tilted angle so that it passes through the focal plane of the microscope. The diameter of the fibre is constant and shown by the vertical white lines.*

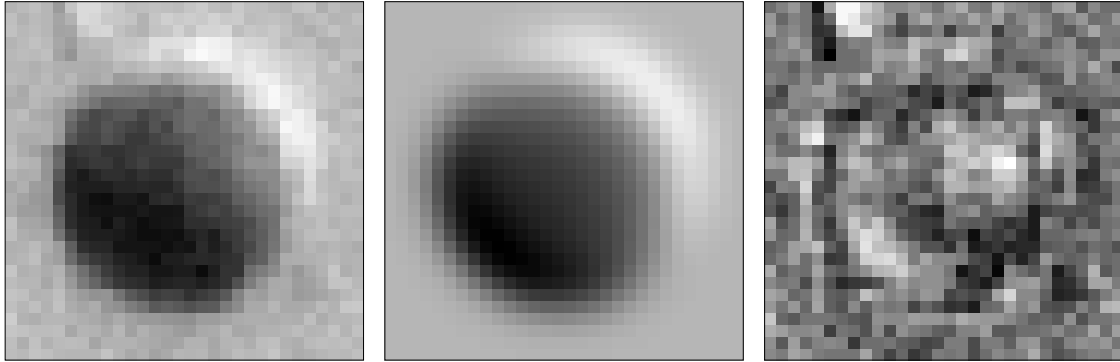


Figure 4: *Differential interference contrast microscope image of a single algal cell (left), together with a fitted model (centre), and the difference between the two images (displayed on a stretched scale with positive residuals displayed as light grey and negative residuals as dark grey).*

qualitative understanding of the optical phenomenon, in practice the situation is more complicated – fibres are neither precisely circular in cross-section, nor are they of constant refractive index, and microscope lenses have flaws. Therefore we resorted to an empirical approach. Glasbey *et al.* (1994) described an algorithm which adjusts estimates of fibre diameters using the intensities of the Becke lines.

Becke lines also pose problems for *automatic focusing* algorithms, which determine when images, or parts of images, are in focus. They assume that lack of focus produces blurred images, and so use focusing criteria which maximise the intensity range or rate-of-change of intensity (see, e.g., Firestone *et al.*, 1991). However, it can be seen in Figure 3, that in the centre of the image where the fibre is in focus, criteria such as these are minimised rather than maximised. It remains an unresolved problem to automatically focus microscope images when Becke lines and blurring phenomena both occur.

Differential interference contrast microscopy

DIC microscopy poses considerable problems for automatic image interpretation because standard methods of image segmentation fail and estimates of cell size are biased. The left-most image in Figure 4 shows a DIC image of a single algal cell. Although this cell is approximately circularly symmetric, its top-right edge appears lighter than the background while the rest is darker. DIC microscopy operates by splitting a beam of light, directing the two halves through the specimen at slightly displaced positions, then recombining them. Where the two beams of light are *in-phase*, after recombination they produce a bright area in the image, whereas when they are *out-of-phase* they cancel out and produce a dark area. DIC is particularly effective in viewing specimens which are almost transparent, because such specimens still change the phase of light passing through them.

We have used *template matching* methods to identify and measure algal, bacterial and fungal cells in images such as Figure 1, involving touching and occluded cells from mixed populations (Young *et al.*, 1995). A key step is the construction of a model of an idealised cell. This is illustrated in the central image of Figure 4. Theory tells us that a spherical cell with radius r , centred at (x_0, y_0) , should produce a DIC image with optical density at location (x, y) given by

$$f(x, y) = \left[a e^{-bt(x,y)} \right] \left[1 + \sin \left(c \frac{dt(x, y)}{dv} \right) \right],$$

where the first bracketed term is the light attenuation in a brightfield microscope and the second term is the DIC effect, $t(x, y)$ denotes the optical thickness of the sphere,

$$t(x, y) = \begin{cases} 2\sqrt{r^2 - (x - x_0)^2 - (y - y_0)^2} & \text{if } (x - x_0)^2 - (y - y_0)^2 \leq r^2 \\ 0 & \text{otherwise,} \end{cases}$$

a , b and c are constants and v ($= y - x$) is the direction of DIC beam displacement. Pixel values in the observed image are given by a convolution with the point spread function of the optical system, which we assume to be Gaussian with variance σ^2 . The seven parameters were estimated to minimise the sum of squares of differences with the left-most image in Figure 4. The fitted model is shown in the central image and the residuals in the right image, from which it can be seen that the model fits very well.

Recovery of depth from focus

Optical microscopes produce poorer images than either electron or confocal microscopes, but they are a lot cheaper, and digital methods can be used to enhance them. For example, *deconvolution* can improve the resolving power, and depth information can be extracted from blur. In optical sectioning, a series of images are taken of a specimen with the optical system focused at different depths perpendicular to the focal plane of the system. Different parts of the specimen are in focus in each image, but these can be obscured or made ambiguous by unfocused information from other parts of the specimen. To illustrate, Figure 5 shows brightfield microscope images of a diatom at four focal planes, a subset of the fourteen images analysed by Lipton and Breen (1995). In the first image the focal plane is above the top surface of the diatom, resulting in a slightly blurred appearance, although the centre of the diatom is less blurred than the rest. The second image is at a slightly lower focal plane and most of the diatom is in focus. However, the edges of the diatom are most in focus in the third and fourth images, which are at still lower focal planes.

For incoherent light (Inoue, 1986), blur is a linear convolution of the optical density of a microscope specimen. Therefore, the pixel value at location (i, j) in the k th image is given by

$$g_{ijk} = \int \int \int w(x, y, z) f(i + x, j + y, k + z) dx dy dz,$$

where $w(x, y, z)$ is the point spread function of the optical system and $f(x, y, z)$ denotes the optical density of the specimen at spatial location (x, y, z) . Many methods, both linear and

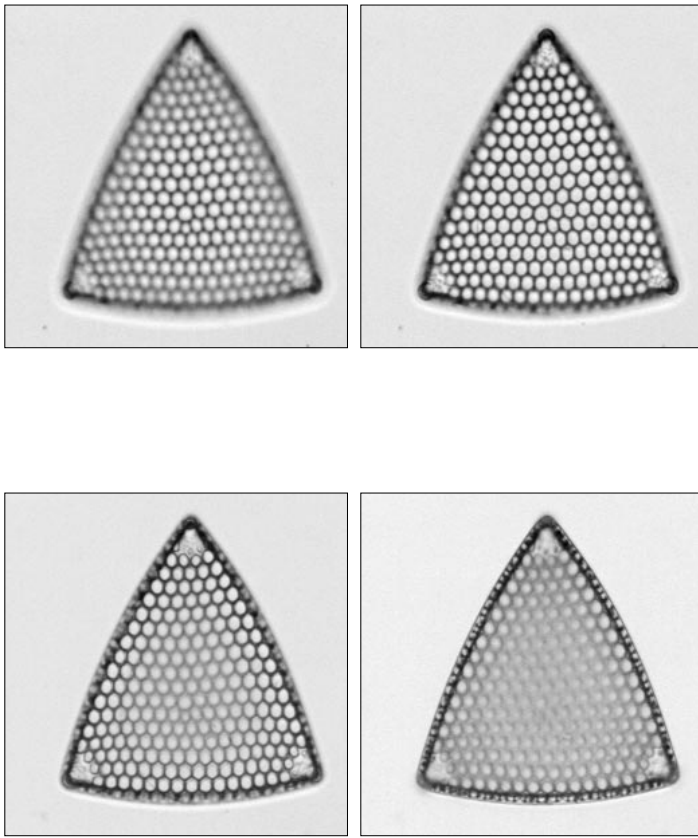


Figure 5: *Diatom imaged in a brightfield microscope at a series of four focal planes.*

nonlinear, have been proposed for recovering f from g , using either a known or estimated w (see, e.g., Preza *et al.*, 1992, Willis *et al.*, 1993).

If a specimen can be considered to be two-dimensional, either because it is a thin section or because it is optically opaque so that only its top surface is imaged, then the extent of blur can be used to infer depth (so-called *depth-from-focus*). It is assumed that

$$f(x, y, z) = \begin{cases} f'(x, y) & \text{if } z = z(x, y) \\ 0 & \text{otherwise,} \end{cases}$$

where $z(x, y)$ denotes the specimen position perpendicular to the focal plane and $f'(x, y)$ denotes the optical density. Darell and Wohn (1990) and Nayar and Nakagawa (1994) both determined $z(i, j)$, for each value of (i, j) , as the image plane (k) in which the output of a high-pass filter applied to g was maximised. Figure 6 shows the recovered three-dimensional top surface of the diatom, obtained from the series of fourteen images using this type of approach, but also with interpolation between imaging planes.

Work is in progress to recover depth information in a less *ad hoc* way by deconvolving g subject to the constraint that f is a two-dimensional surface, thereby combining depth-from-focus and deconvolution into a single algorithm. The problem can be formulated as that of minimising

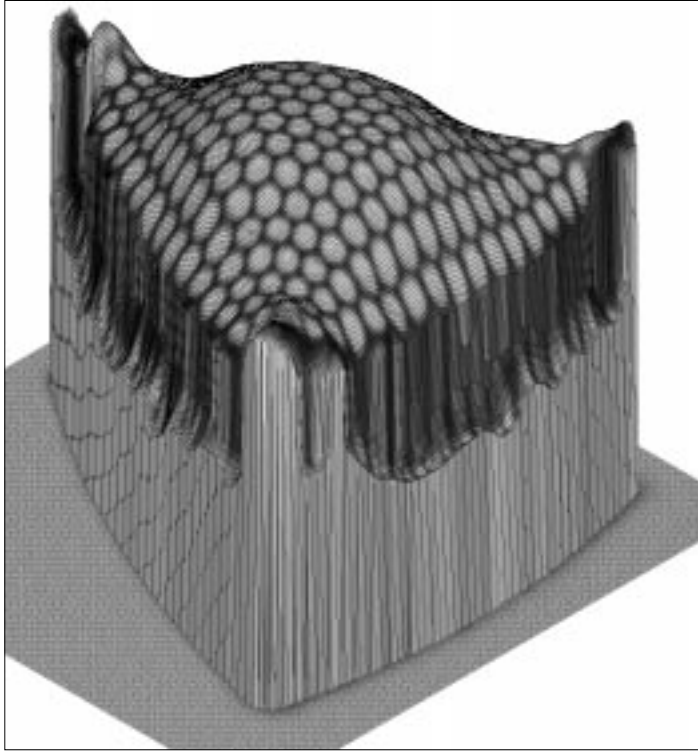


Figure 6: *Reconstructed three-dimensional top surface of the diatom, obtained from a series of images at fourteen focal planes.*

the sum of squares:

$$\sum_i \sum_j \sum_k \left(g_{ijk} - \sum_x \sum_y w(x, y, z(x, y) - k) f'(i + x, j + y) \right)^2$$

with respect to f' and z , though a roughness penalty may also need to be included in the objective function. In a series of raster scans, for each value of (x, y) in turn, $f'(x, y)$ is updated and $z(x, y)$ is changed by a small amount and the effects on the sum of squares are evaluated. Changes in depth are adopted according to a simulated annealing schedule (to avoid being trapped in local minima) until no further reductions in the sum of squares can be made.

Acknowledgements

I am grateful to Angus Russel, Nick Martin and Ed Breen for permission to use their images in this paper. The work was supported by funds from the Scottish Office Agriculture, Environmental and Fisheries Department.

References

Darell, T. and Wohn, K. (1990). Depth from focus using a pyramid architecture. *Pattern*

Recognition Letters, **11**, 787-796.

Firestone, L., Cook, K., Culp, K., Talsania, L. and Preston Jr., K. (1991). Comparison of autofocus methods for automated microscopy. *Cytometry*, **12**, 195-206.

Glasbey, C.A., Hitchcock, D., Russel, A.J.F. and Redden, H. (1994). Towards the automatic measurement of cashmere-fibre diameter by image analysis. *Journal of the Textile Institute*, **85**, 301-307.

Glasbey, C.A. and Horgan, G.W. (1995). *Image Analysis for the Biological Sciences*. Wiley, Chichester.

Inoue, S. (1986) *Video microscopy*. Plenum Press, New York.

Lipton, A. and Breen, E.J. (1995). On the use of local statistical properties in focusing microscopy images. *Microscopy Research and Techniques*, **31**, 326-333.

Nayar, S.K. and Nakagawa, Y. (1994). Shape from focus. *IEEE Transactions on Pattern Analysis and Machine Intelligence*, **16**, 824-831.

Preza, C., Miller, M.I., Lewis, J.T. and McNally, J.G. (1992). Regularized linear method for reconstruction of three-dimensional microscopic objects from optical sections. *Journal of the Optical Society of America, A*, **9**, 219-228.

Slyter, E.M. and Slyter, H.S. (1992). *Light and Electron Microscopy*. Cambridge University Press, Cambridge.

Willis, B., Roysam, B., Turner, J.N. and Holmes T.J. (1993). Iterative, constrained 3-D image reconstruction of transmitted light bright-field micrographs based on maximum likelihood estimation. *Journal of Microscopy*, **169**, 347-361.

Young, D., Glasbey, C.A., Gray, A.J. and Martin, N.J. (1995). Cell identification in differential interference contrast microscope images using template matching. *Scandinavian Image Analysis Conference - 95SCIA*, Uppsala, Sweden, June 1995, 199-208.